



OPEN ACCESS

EDITED BY
Giuseppe Mandaglio,
University of Messina, Italy

REVIEWED BY
Habib Elhouichet,
Tunis El Manar University, Tunisia
Francesco Caridi,
University of Messina, Italy

*CORRESPONDENCE
H. O. Tekin,
tekin765@gmail.com
Antoaneta Ene,
Antoaneta.Ene@ugal.ro

SPECIALTY SECTION
This article was submitted
to Nuclear Physics,
a section of the journal
Frontiers in Physics

RECEIVED 26 October 2022
ACCEPTED 21 November 2022
PUBLISHED 05 December 2022

CITATION
ALMisned G, Baykal DS, Kilic G, Ilik E,
Zakaly HMH, Ene A and Tekin HO (2022),
A critical evaluation on nuclear safety
properties of novel cadmium oxide-rich
glass containers for transportation and
waste management: Benchmarking
with a reinforced concrete container.
Front. Phys. 10:1080354.
doi: 10.3389/fphy.2022.1080354

COPYRIGHT
© 2022 ALMisned, Baykal, Kilic, Ilik,
Zakaly, Ene and Tekin. This is an open-
access article distributed under the
terms of the [Creative Commons
Attribution License \(CC BY\)](https://creativecommons.org/licenses/by/4.0/). The use,
distribution or reproduction in other
forums is permitted, provided the
original author(s) and the copyright
owner(s) are credited and that the
original publication in this journal is
cited, in accordance with accepted
academic practice. No use, distribution
or reproduction is permitted which does
not comply with these terms.

A critical evaluation on nuclear safety properties of novel cadmium oxide-rich glass containers for transportation and waste management: Benchmarking with a reinforced concrete container

Ghada ALMisned¹, Duygu Sen Baykal², G. Kilic³, E. Ilik³,
Hesham M.H. Zakaly^{4,5}, Antoaneta Ene^{6*} and H. O. Tekin^{7,8*}

¹Department of Physics, College of Science, Princess Nourah Bint Abdulrahman University, Riyadh, Saudi Arabia, ²Istanbul Kent University, Vocational School of Health Sciences, Medical Imaging Techniques, Istanbul, Türkiye, ³Eskisehir Osmangazi University, Faculty of Science, Department of Physics, Eskisehir, Türkiye, ⁴Institute of Physics and Technology, Ural Federal University, Yekaterinburg, Russia, ⁵Physics Department, Faculty of Science, Al-Azhar University, Assiut, Egypt, ⁶Department of Chemistry, Physics and Environment, INPOLDE Research Center, Faculty of Sciences and Environment, Dunarea de Jos University of Galati, Galati, Romania, ⁷Medical Diagnostic Imaging Department, College of Health Sciences, University of Sharjah, Sharjah, United Arab Emirates, ⁸Istinye University, Faculty of Engineering and Natural Sciences, Computer Engineering Department, Istanbul, Türkiye

We examine the nuclear safety properties of a newly designed cadmium oxide-rich glass container for nuclear material to a bitumen-reinforced concrete container. Individual transmission factors, detector modelling, and energy deposition (MeV/g) in the air are calculated using MCNPX (version 2.7.0) general purpose Monte Carlo code. Two container configurations are designed with the material properties of cadmium dioxide-rich glass and Concrete + Bitumen in consideration. First, individual transmission factors for ⁶⁰Co and ¹³⁷Cs radioisotopes are calculated. To evaluate potential environmental consequences, energy deposition amounts in the air for ⁶⁰Co and ¹³⁷Cs are also determined. The minimum gamma-ray transmission rates for two container types are reported for a cadmium dioxide-rich glass container. In addition, the quantity of energy deposition is varied depending on the container type, with a lower value for cadmium dioxide-rich glass container. The 40% cadmium dioxide-doped glass container provides more effective safety than the Cement + Bitumen container, according to the overall findings. In conclusion, the utilization of cadmium dioxide-doped glass material along with its high transparency and advanced material properties may be a significant and effective option in areas where concrete is required to assure the safety of nuclear materials.

KEYWORDS

nuclear safety, container, MCNPX, CdO, glasses

Introduction

Each year, approximately 15 million containers of radioactive material are carried around the world [1]. Radioactive materials and nuclear fuel packages are transported globally through ships, roads, planes, and railways. In the United States, only around 250,000 out of a total of 3,000,000 radioactive parcels distributed annually include waste from nuclear power reactors in the country, and only about 25–100 contain burnt fuel. The US Department of Transportation reports that the typical distance travelled by a shipment of radioactive material is around 55 km, far less than the average distance travelled by shipments of all hazardous chemicals, which is about 185 km [1]. The transportation of all materials is controlled by efficient, safe, and reliable guidelines from mining to manufacturing, storage, and usage—transportation of radioactive material by containers used for storage and transportation to prevent any leak into the environment. Transportation of nuclear elements and radioactive materials is taken seriously and strictly according to the best guidelines developed by the International Atomic Energy Agency (IAEA) and followed by each courtier. IAEA published 1961 the international regulation for transportation of radioactive materials with the latest revision published in 2018 [2–4]. The importance of this regulation is to protect the environment and humans from the radiation effect during transportation. In addition, the regulation covers routine and emergencies during transportation. The basic element of transportation is the design of the package and container, which should prevent contamination, criticality, and damage. Personnel and the public involved in transportation or on the route should be protected. The containers should be shielded to eliminate the radiation risk. Dual-purpose containers, suitable for both storage and transport of used nuclear fuel, are frequently used to reduce the risk of handling highly radioactive materials. Different materials are used to shield radioactive and nuclear containers such as concrete and lead because of durability, expenses, ability to attenuate different radiation photons and design flexibility. The shielding material chives depend on the radiation type, activity, and the accepted dose outside the container. Without emitting additional dangerous radiation, an effective shield will result in a substantial energy loss at a small penetration distance. Concrete is a good and adaptable shielding material; therefore, it is often used to protect nuclear power plants, particle accelerators, research reactors, Nuclear Medicine HOT labs, and even medical institutions. It is a low-cost material that's easy to work with and can be designed in different shapes. In addition, because it is made up of light and heavy elements, it has strong nuclear characteristics for photon and neutron attenuation. The density of concrete and lead shielding made it difficult to be used in the shielding of radioactive transportation containers. This led to thinking about novel, cost-effective, light materials with chemical and physical characteristics that can be used in storage and

transportation containers. Researchers used the nanoparticles to the concrete mixture to improve the structural and mechanical characteristics. The study of gamma and neutron radiation absorption in shielding materials has long been a topic of interest in the discipline of radiation physics. For example, most of the previous research has focused on photon attenuation coefficients rather than the air-karma. Some recent novel concept examinations, however, have provided a more thorough report by comparing and evaluating the air-kerma and the individual radiation reduction of these newly developed containers. Tekin et al., conducted a study utilizing a sophisticated Monte Carlo method to examine the impact of strengthening degree on the protective qualities of Bi₂O₃ heavy metal oxide-doped glassy portable containers [5]. There was a significant difference between the levels of protection supplied by heavy oxide-containing glass portable containers and those offered by reinforced concrete containers. Meanwhile, research conducted on glass materials, particularly in the past few years, has shown that these materials are appropriate for usage in radiation fields due to their radiation absorption qualities as well as their mechanical and optical capabilities [6–10]. Transition metal oxide (TMO)-doped glasses have been used as optoelectronic components in a variety of fields [11–14]. As known, CdO, which is doped in both glasses and thin films, is one of them. In the literature, cadmium dioxide (CdO) is doped to base glasses to give them color, increase moisture resistance, and improve other optical characteristics. In other respect, the fact that it is a high-density compound allows CdO-doped glasses to be alternative materials in the field of radiation shielding [15]. Since the high density of radiation shielding materials significantly changes the properties of the relevant material, CdO is an important oxidized compound in this and similar studies. In our previous studies, P₂O₅-TeO₂-ZnO glasses containing CdO in different ratios [16–19] optical, physical and radiation shielding properties are emphasized. These characterizations are handled at low ratios of CdO and high ratios of CdO. Experimental neutron shielding characterization using ¹³³Ba radioisotope and experimental gamma-ray using a²⁴¹Am/Be neutron source, compared to glasses with low CdO [19], samples with high CdO [18] showed better results. In fact, in these studies, it was determined that the sample containing 40 mol% CdO, coded as C40, gave the most effective result. The fact that the sample with the highest density in terms of physical properties is C40, reveals the dependence of radiation shielding properties on sample density. The major objective of this study is to report initial findings of our novel work on the design of some CdO-rich high-density quaternary glass samples that were synthesized by our group with the concept of nuclear material container in consideration. In presenting the findings obtained from the study and the used methodologies to the readers, the technical parameters of the simulation, the details of the input code written, the detection types used, the comparison phase, and the results obtained will be discussed in detail. This research has

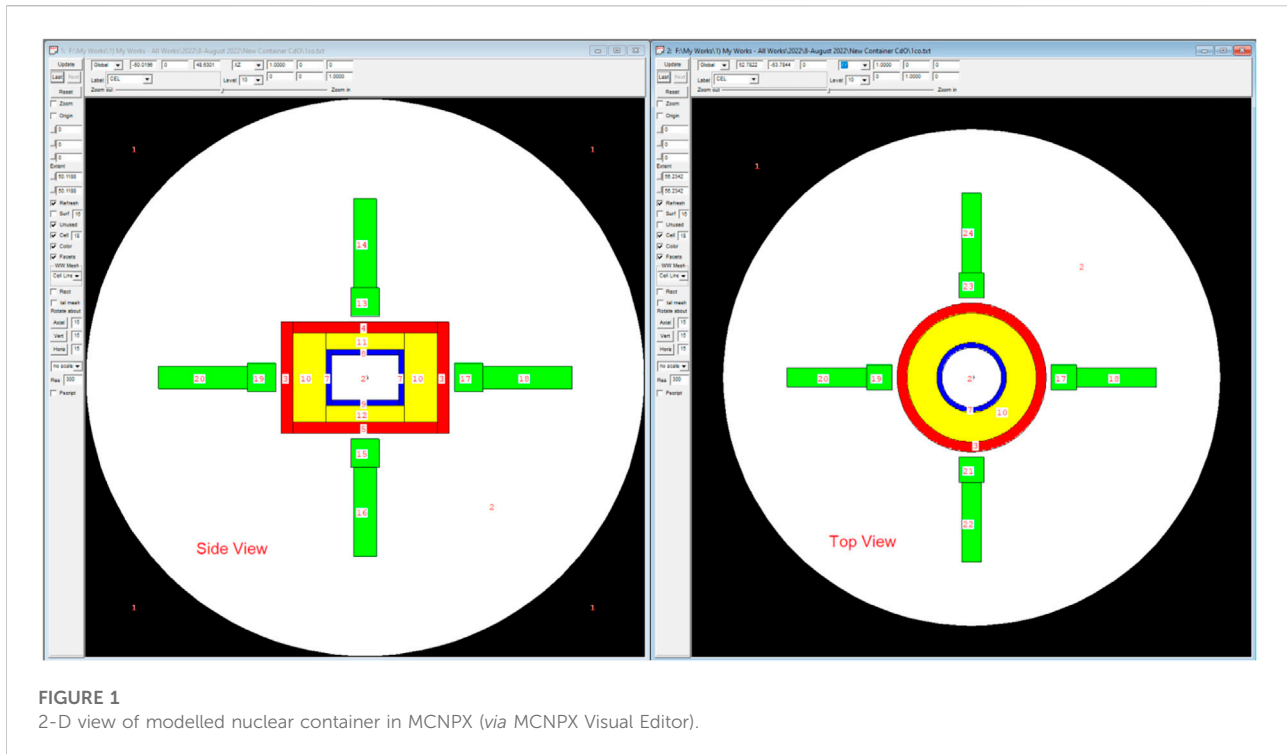


FIGURE 1
2-D view of modelled nuclear container in MCNPX (via MCNPX Visual Editor).

the potential to increase our understanding of the role glass materials might play in the nuclear industry and engineering sectors.

Materials and methods

C40 glass sample synthesis

In previous studies, the C40 sample, which is one of the glass samples synthesized due to the P_2O_5 - TeO_2 - ZnO / CdO structure [16–19], was obtained by melt-quenching method. C40 sample with initial composition of 20 P_2O_5 .30 TeO_2 .10 ZnO .40 CdO (in mol%) was melted in a platinum crucible at 900°C using high purity chemicals and annealed at approximately 385°C to balance the internal forces. Detailed information on sample synthesis and sample shaping is given in our previous work [16–19].

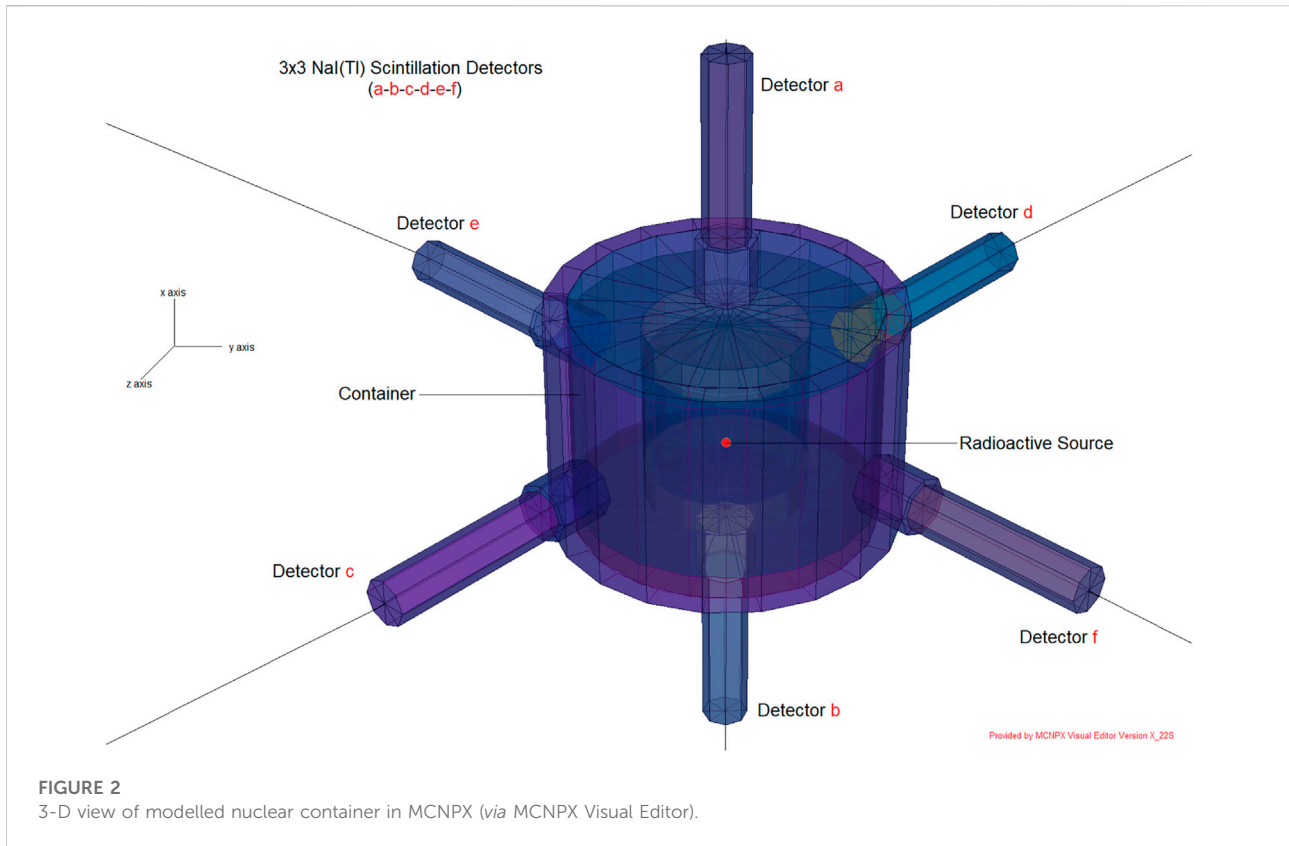
Definition of input file in MCNPX

Studies using the MCNPX code should consider the proper steps of preparing the INPUT file in accordance with the code structure. In fact, there are three main defining areas such as CELL, SURFACE, and DATA cards that should be accomplished before the simulation process. The research begins by defining the bounds of each cellular structure in terms of geometric boundaries. Figure 1 is a two-dimensional illustration of the

modelled transportable container. As can be seen, the geometry of an isotropic point source is placed at the simulation volume's origin (i.e., 0, 0, 0). The chemical compositions of the glass container and compared concrete container were used to design a novel cellular structure for the transportable containers. Finally, an air cell encompassing the glass container was specified in the input data. The air cell has been shielded from the environment by an attenuator layer since the major objective of this study was to quantify the total energy released into the surrounding air cell (see Figure 2). This was achieved by simulating the release of radiation into four distinct containers using the energy released into the air by the radioactive decay of ^{60}Co and ^{137}Cs radioisotopes administered within the container. In order to assure the reliability of the surrounding air environment for any radiation leakage condition, six 3×3 inch NaI(Tl) scintillation detectors have been distributed around the simulation regions. Our purpose for developing these six detectors (from a to f) was to ensure that the air environment around the container is properly sealed off from the external simulation environment and that the air-kerma to be measured is truly a component of the air around the container.

Benchmarking of individual transmission factor values (TFs)

In addition to understanding the radiation absorption characteristics of the materials, knowing the quantitative



attenuation qualities of the materials against the source of the gamma ray helps improve the materials' engineering uses. This is accomplished by dividing the intensity of the primary gamma rays emitted by the source by the intensity of the secondary gamma rays remaining after passing through the absorbent material. This phenomenon is also referred to as the transmission factor (TF) of the material [10, 20, 21]. In this work, the first step of comparison included estimating the absorption in TF of a glass container containing CdO and a concrete container containing Bitumen against gamma rays emitted by ⁶⁰Co and ¹³⁷Cs sources.

Using the F4 Tally Mesh placed on the front and back of the container section, the quantiles of the gamma rays emitted by the source and the secondary gamma rays remaining on the other side of the container were determined using following formula.

$$TF = \text{Counted photon flux in } (F4)_2 / \text{Counted photon flux in } (F4)_1 \quad (1)$$

Where,

(F4)₁: Designed F4 Tally Mesh for primary photons

(F4)₂: Designed F4 Tally Mesh for secondary photons

Meanwhile, the simulation design shown in Figure 3 was constructed specifically for this comparative phase by temporarily modifying the primary code design. According to the code hierarchy, a few lines of code are written to do just

the counts for the two different Tally Meshes (see Figure 3) throughout the modification process. For the simulation, TF values were estimated for three different energies: 1.17 MeV and 1.33 MeV for the ⁶⁰Co source and 0.663 MeV for the ¹³⁷Cs source.

Determination cadmium oxide-rich glass sample (C40)

CdO-doped glasses are of special interest due to their usefulness in several nonlinear optical material applications. During glass production, the structure and properties of the glass are largely determined by the function of the constituent's oxide as a network modifier or network former [22, 23]. Previously, the maximum possible CdO additive amount has been studied in terms of enhancing the gamma-ray attenuation properties. The initial findings showed that 40% mole CdO additive (i.e., C40 sample) would significantly improve the overall gamma-ray attenuation properties [18, 19] and heavy charged particle attenuation [16, 17] of P₂O₅-TeO₂-ZnO ternary glass system. The impact of these glasses on the quantity of dose received in air based on attenuation in circumstances where several regularly used radioisotope energies have an isotropic distribution has not

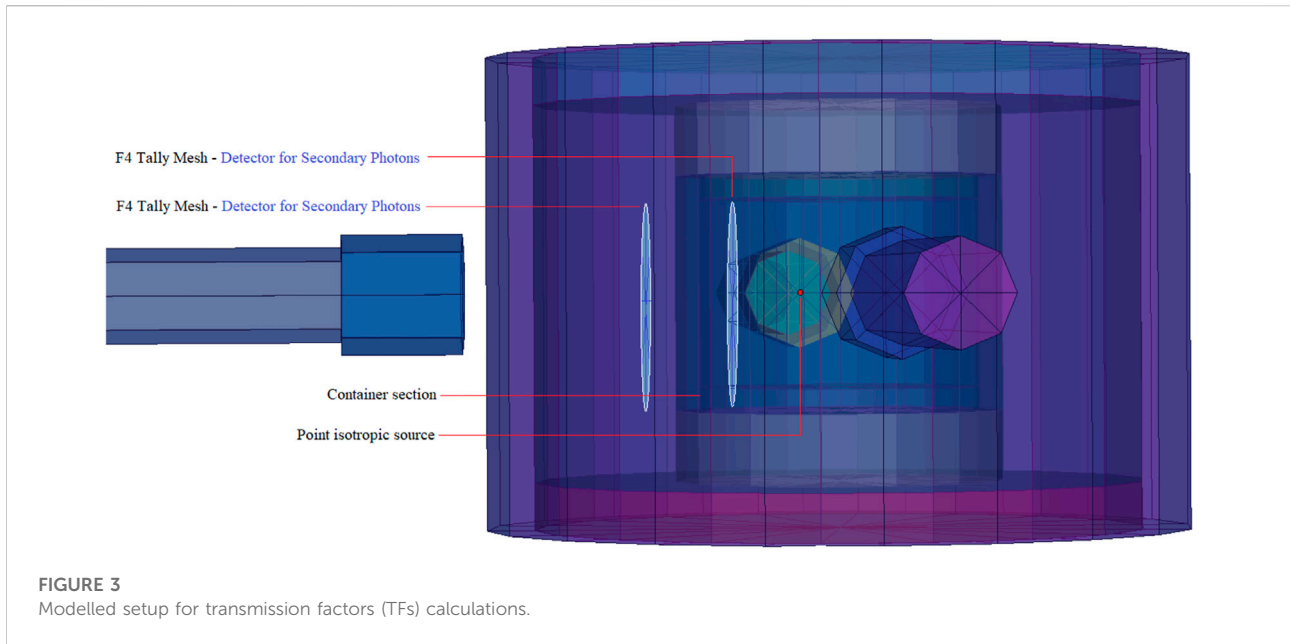


FIGURE 3
Modelled setup for transmission factors (TFs) calculations.

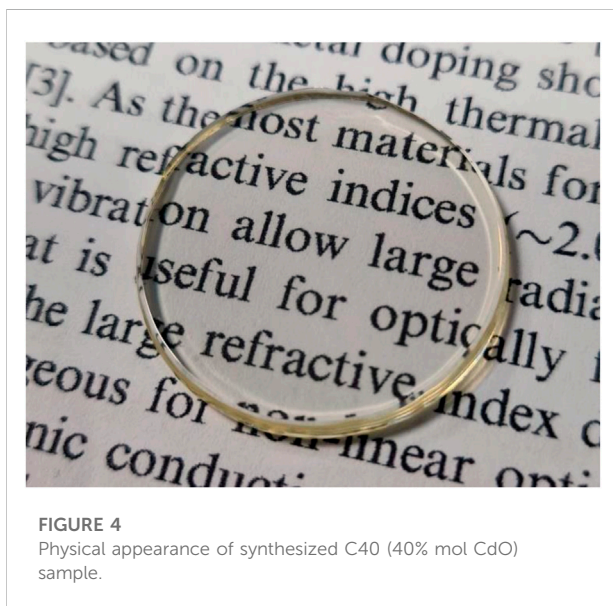


FIGURE 4
Physical appearance of synthesized C40 (40% mol CdO) sample.

appearance of the manufactured C40 glass sample along with its excellent transparency is shown in Figure 4.

Calculation of deposited energy amount in the air

We constructed four distinct INPUT files, one for each of two containers separately for two distinct radioisotopes. After the INPUT files were created, they were analysed one by one for a total of 10^8 particle numbers before the output files were recorded. Figure 2 is a 3-D representation of the modelled container as it appears in the MCNPX visual editor. The radioisotope is contained in a cylindrical cylinder with a closed top and bottom. For the purposes of this research, the output recording functionality of the MCNP code, namely F6 TALLY MESH, is used. Total energy deposited in a cell may be calculated as MeV/g or jerks/g using F6 TALLY MESH. In this study, three unique cellular volumes were implanted using definitions from the F6 TALLY MESH. Three distinct cellular volumes are shown in Figure 1; they are Cells 10, 11, and 12, as well as the air around the portable glass container. After each simulation cycle is complete, the output file is analyzed for the quantities of energy deposited in these 3 cells, and the total is recorded. Therefore, during each simulation cycle, the total amount of energy deposited in the 3 cell volumes of air around the container was obtained. Meanwhile, Figure 1 also depicts the placement of scintillation detectors around the container. Cells 19, 13, 15, and 17 in Figures 1,2 were defined as NaI(Tl) detectors, and definitions were constructed that would allow

been studied. Lack of examine this condition limits the observation and overall understanding of the consequences of a potential application of glass materials in the nuclear waste management process, one of the most promising applications of glass materials. The primary objective of this research is to represent the ternary glass sample with 40% mole CdO in the idea of a container and to make some significant contributions to its industrial use and engineering side utilizing numerous detection techniques. The physical

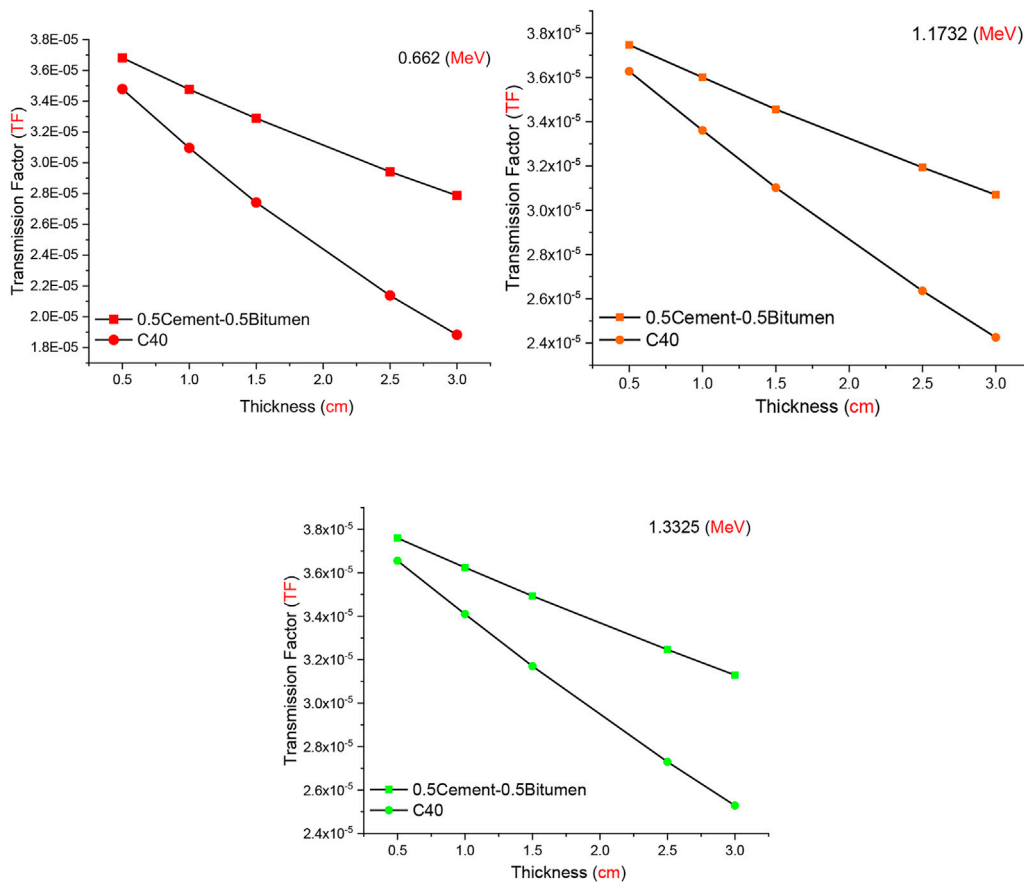


FIGURE 5
Variation of TFs as a function of material thickness for 0.5 Cement-0.5 Bitumen and C40 glass containers.

any gamma ray response function to be observed in these cells [24, 25].

Results and discussions

Individual transmission performances of bitumen concrete and C40 sample

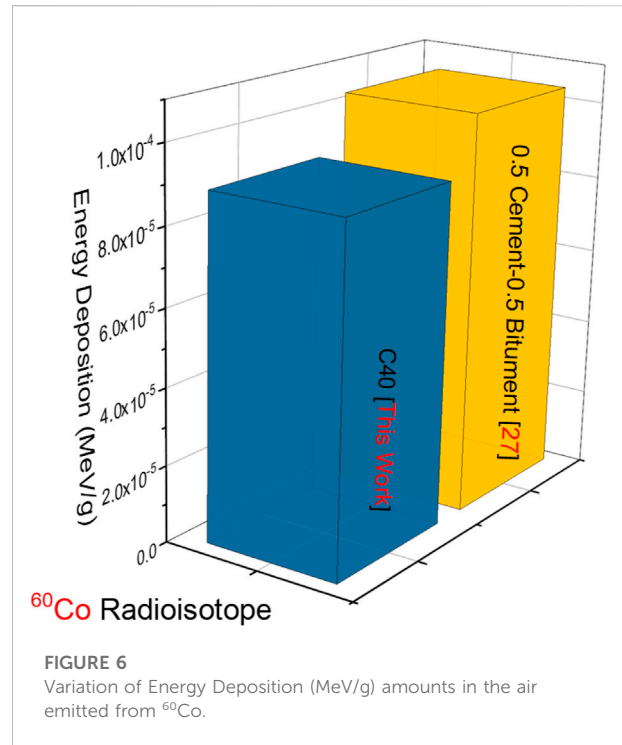
The first phase of the study comprised of defining 2 separate detection areas for the inner and outer segments of the modelled container geometry and, as a result, assessing the individual transmission factors by determining the ratio of the primary gamma rays emitted by the source to the secondary gamma rays passing through the cross section of the container. In this phase, the container’s body material was determined based on the chemical composition and densities of bitumen-added concrete [26] and C40 glass [16, 18] sample. The source energy was computed for three distinct gamma energies 0.662 MeV, 1.1723 MeV, and 1.3325 MeV emitted by ¹³⁷Cs

and ⁶⁰Co radioisotopes. The variations of the transmission factors (TFs) were then obtained as a function of the thickness. Figure 5 depicts the behavioural changes in TF values for bitumen-added concrete and C40 glass sample for three distinct radioisotope energies at different thicknesses. As seen in the graph, the TF values for each of the three energy values tended to decrease as the material thickness increased. This is a naturally occurring phenomenon that can be anticipated for almost any kind of material, since the quantity of absorbed photons increases as the thickness of the material increases. Nonetheless, a rise in the TF factor values was also found for both materials as the energy increased. In other words, in conjunction with the increase in radioisotope energy, the gamma ray’s penetrating qualities and the intensity of secondary gamma-rays increased. On the other hand, as shown in equation 1, a decrease in the quantity of secondary gamma rays would similarly lower the TF value. This may be explained by the fact that the quantity of gamma rays that can travel through thick materials is less than that of thin materials. Consequently, the TF values obtained for the 40% CdO added

C40 sample were lower for each of the three radioisotope energies than the TF values found for the Bitumen added concrete sample. This difference has become more pronounced at 3 cm, which is the thickest value, particularly for the TF values that vary with the increase in material thickness. According to these observations, the transmission factor properties of the C40 sample are much more progressive and superior to those of the concrete material containing bitumen.

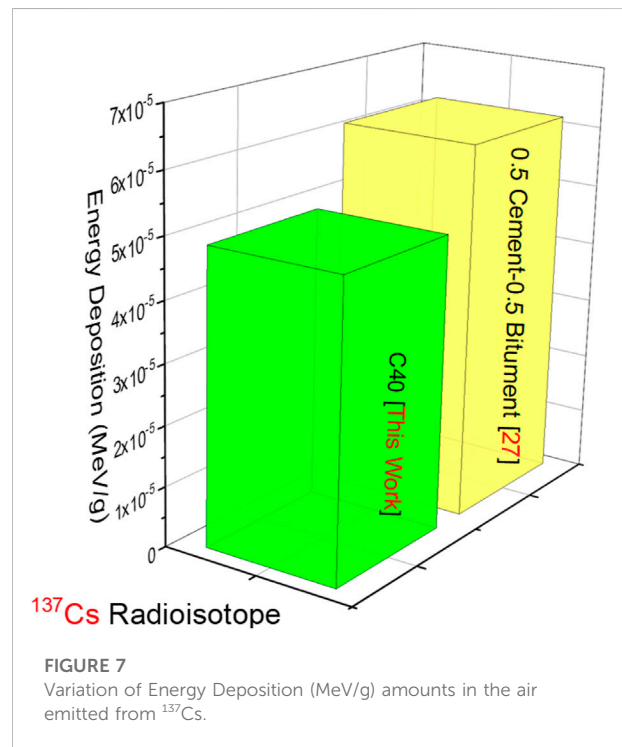
Energy deposition in the air

The quantity of energy absorbed by the air is an additional crucial parameter to examine for radiation protection. A solid understanding of this parameter allows for the quantification of the energy that is absorbed per unit of air by identifying the amount of radiation to which the environment is exposed. Personal dosimeters used in radiation fields, on the other hand, execute their functions based on the quantity of ionized radiation in the air, making this parameter essential for dosimetry research. The superior absorption capabilities of the material that accomplishes the radiation absorption process contribute to the smallest quantity of absorbed radiation in the air. By selecting more efficient materials for the shielding technique to be applied to the radioactive material, it will be less likely that more of the source’s main radiation will be absorbed by the material and escape into the air. In the second phase of this investigation, it was essential to define and compare the amount of energy released by gamma rays from radioisotopes placed in C40 and Cement + Bitumen containers after primary reduction. For this reason, the container structure was modelled independently for C40 and Cement + Bitumen, and the cumulative energy deposition in the surrounding cells (see Cell 10 and Cell 11) was calculated separately. Apparently, for the accuracy of this calculation, it is required to ensure that Cells three and four surrounding the air environment do not transmit radiation to the back. Due to this, appropriate designs have been created to offer a response function for the six distinct NaI(Tl) detectors shown in Figure 2. Before beginning the second phase of research, the response function of these detectors was checked in a test simulation, and no count was recorded. This demonstrated that cells three and four offered the highest isolation from the outside air. In other words, the air environment around the container has the same quantitative characteristics as the radiation extracted from the container for testing purposes, and there were no data errors beyond the context of the research. The following phase was calculating the quantity of energy absorbed by the air using the F6 Tally Mesh feature of the MCNPX algorithm. Figure 6 and Figure 7 demonstrates the fluctuation of the energy absorbed in the air by two distinct radioisotopes such as ⁶⁰Co and ¹³⁷Cs for the C40 and Cement + Bitumen containers, respectively. As seen in the graph, the quantity



⁶⁰Co Radioisotope

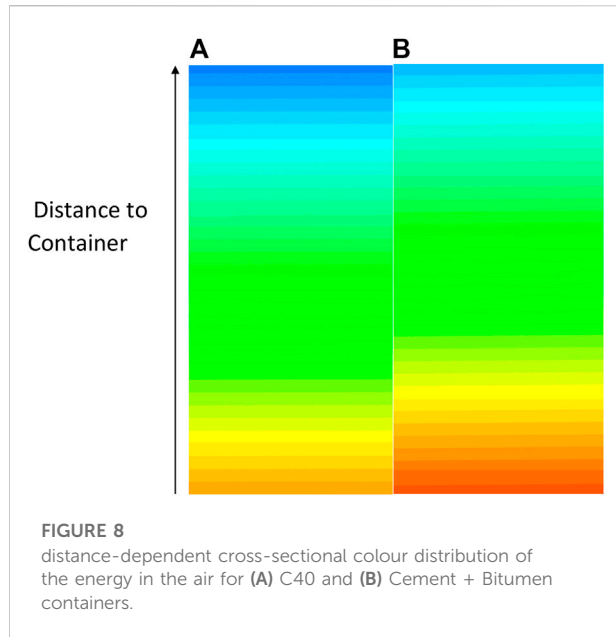
FIGURE 6 Variation of Energy Deposition (MeV/g) amounts in the air emitted from ⁶⁰Co.



¹³⁷Cs Radioisotope

FIGURE 7 Variation of Energy Deposition (MeV/g) amounts in the air emitted from ¹³⁷Cs.

of energy each radioisotope release into the air has changed depending on their energy values. Since the average amount of energy of the ¹³⁷Cs radioisotope is less than that of the ⁶⁰Co radioisotope, its exposure to the air and, thus, the amount of



energy absorbed in the air are estimated to be lower in both containers compared to ^{60}Co . In addition, the quantity of energy absorbed in the air changed between C40 and Cement + Bitumen containers containing the same radioisotopes. In situations when the C40 container was used, both ^{60}Co and ^{137}Cs radioisotopes absorbed less energy from the air. This demonstrates that the absorption processes of primary gamma from C40 are more efficient than the Cement + Bitumen container, and a significant change in air transmission has been detected. This finding indicates that a more effective nuclear protection operation may be carried out when the C40 container is employed as compared to a concrete container with bitumen additive. In addition, the distance-dependent cross-sectional colour distribution of the energy received in the air by both containers is seen in Figure 8. As the distance between the container and the air increases, the quantity of energy absorbed in the air by both containers decreases. However, the quantity of energy that occurs at the point where the C40 container makes first contact with air is less than the amount that arrives at the same point for the Cement + Bitumen container. As illustrated in Figure 8, the blue regions are more prominent for C40, and a more minimum energy distribution is found for C40. This condition is also a multiple confirmation of the findings obtained from the TF values and the energy absorbed in the air (MeV/g) measurements. Considering the realistic application conditions of the glass container containing 40% CdO, the obtained findings suggest that Cement + Bitumen has more beneficial features than the container and will offer more advantageous and dependable conditions for the transport and storage of nuclear resources.

Conclusion

During the use of nuclear energy, security is recognized as the most important factor. Any nuclear application for which the security requirements are not optimized poses a risk. This application is relevant not just for energy production issues, but also for medical operations involving physical radiation sources, particularly of the nuclear medicine. The degree to which a radioactive substance is shielded before, during, and after use, as well as during transportation, determines its safety. This is valid even after the disposal of radioactive materials, and circumstances of maximal shielding and protection must be provided anytime radiation is present. At this point, containers for nuclear material are extremely important. The use of such materials during storage, transportation, and post-use storage prevents the direct or indirect contact of radioactivity with live biological tissues *via* the release of radioactive particles into the air, water, or soil. This study's objective was to simulate application-based properties in their most realistic form by comparing concrete, a classic container material, with heavy glass, which has established a prominent position in the literature as a new generation of nuclear shielding materials. The application of Monte Carlo simulations to problems of radiation transport not only provides a great deal of scientific ease, but also allows the implementation of experimental or clinical research with more efficiency. Radiation research is not always a simple operation. These investigations must be conducted within in the frame by government regulations and in compliance with the laws. On the other hand, radiation experiments are quite expensive. As is well-known, the incorrect or unintentional usage of radiation may have highly hazardous health consequences. For this reason, comprehensive simulation procedures for the experiment to be conducted or the scenario to be implemented provide great safety, environmental, and financial benefits. This study's simulation enabled us to comprehend the radiation absorption properties of the designed glass container, as well as where optimization studies are required prior to production design, or how the existing situation may be enhanced. The best materials for radiation shielding were found to be $\text{P}_2\text{O}_5\cdot\text{TeO}_2\cdot\text{ZnO}$ glasses with 40% mole percent CdO doped in the previously prepared series. The glass density was markedly increased by the maximum CdO contribution, resulting in a high-density C40 sample that was denser than the majority of commercial glasses. The C40 sample was therefore the main focus of this investigation. The assessment of the specific radiation absorption characteristics of cadmium-doped glasses was the motivation for this material to be designed in a practical container concept and various application-based parameters to be investigated. Multiple assessment parameters acquired as

a consequence of the investigation revealed that the 40% CdO-doped glass containers offer more effective protection than the advanced Cement + Bitumen containers. Obviously, the advantage shown by the glass container containing CdO is not limited to radiation absorption alone. Other benefits that might be supplied in comparison to typical concrete containers include its greater optical permeability, the enhanced advantages of glass materials against corrosion, and its superior resistance to breakage and material defects. In conclusion, the use of CdO doped glass materials can be an important and effective alternative in areas where concrete materials are used to ensure nuclear material safety. Although the application of advanced simulation methods in the current study offers several advantages, it is necessary to address some limitations. The reliability and validity of simulation studies performed with codes such as MCNP, Geant4, EGSnrc, and FLUKA used for radiation transport have been ensured in terms of both the physics lists and program libraries, yet the information provided by the real experimental conditions is always more valuable. The simulation should be assessed in a preliminary preparation stage for preliminary manufacturing studies. According to their elemental percentages and densities, the material, air, and other experimental components established in the simulation environment are characterized as perfect materials. In fact, this is not the case, and it must be kept in mind that every material has a certain number of internal fractures, deformations, and other conditions that may prevent the attainment of the most accurate outcome.

Data availability statement

The raw data supporting the conclusion of this article will be made available by the authors, without undue reservation.

References

1. Ratin AS, Mithel MFH, Rishad AS, Nitu TAK. Radioactive waste management of nuclear power plant. *Int J Renew Energ Res.* (2014) 3(7):1–10.
2. International Atomic Energy Agency. *Format and content of the package design safety report for the transport of radioactive material, IAEA safety standards series No. SSG-66.* Vienna, Austria: IAEA (2022). Available at: <https://www.iaea.org/publications/14800/format-and-content-of-the-package-design-safety-report-for-the-transport-of-radioactive-material> (Accessed October 15, 2022).
3. International Atomic Energy Agency. *Advisory material for the IAEA regulations for the safe transport of radioactive material (2018 edition), IAEA safety standards series No. SSG-26 (rev. 1).* Vienna, Austria: IAEA (2022). Available at: <https://www.iaea.org/publications/14685/advisory-material-for-the-iaea-regulations-for-the-safe-transport-of-radioactive-material-2018-edition> (Accessed October 15, 2022).
4. International Atomic Energy Agency. *Preparedness and response for a nuclear or radiological emergency involving the transport of radioactive material, IAEA safety standards series No. SSG-65.* Vienna, Austria: IAEA (2022). Available at: <https://www.iaea.org/publications/14678/preparedness-and-response-for-a-nuclear-or-radiological-emergency-involving-the-transport-of-radioactive-material> (Accessed October 15, 2022).

Author contributions

GA: Conceptualization, calculations, writing. DS: Calculations, data analysis. GK: Measurements, writing. EI: Measurements, writing. HZ: Writing, data analysis. AE: Writing, data analysis. HT: Writing, calculations, supervision.

Funding

The authors extend their appreciation to the Deputyship for Research and Innovation, Ministry of Education in Saudi Arabia for funding this research work through the project number RI-44-0003.

Acknowledgments

The author AE acknowledges the support of Dunarea de Jos University of Galati, Romania, through the grant no. RF 3621/2021.

Conflict of interest

The authors declare that the research was conducted in the absence of any commercial or financial relationships that could be construed as a potential conflict of interest.

Publisher's note

All claims expressed in this article are solely those of the authors and do not necessarily represent those of their affiliated organizations, or those of the publisher, the editors and the reviewers. Any product that may be evaluated in this article, or claim that may be made by its manufacturer, is not guaranteed or endorsed by the publisher.

5. Tekin HO, Rainey C, Almisned G, Issa SAM, Akkus B, Zakaly HM. Heavy metal oxide added glassy portable containers for nuclear waste management applications: In comparison with reinforced concrete containers. *Radiat Phys Chem Oxf Engl* 1993 (2022) 201:110449. doi:10.1016/j.radphyschem.2022.110449
6. Issa SA, Ali AM, Tekin HO, Saddeek YB, Al-Hajry A, Algarni H, et al. Enhancement of nuclear radiation shielding and mechanical properties of YBiBO₃ glasses using La₂O₃. *Nucl Eng Tech* (2020) 52(6):1297–303. doi:10.1016/j.net.2019.11.017
7. Almisned G, Bilal G, Rammah Y, Issa SA, Kilic G, Zakaly HM, et al. Mechanical properties, elastic moduli, and gamma radiation shielding properties of some zinc sodium tetraborate glasses: A closer look at ZnO/CaO substitution. *J Electron Mater* (2021) 50(12):6844–53. doi:10.1007/s11664-021-09246-3
8. Lakshminarayana G, Issa SA, Saddeek YB, Tekin HO, Al-Buriah MS, Dong MG, et al. Analysis of physical and mechanical traits and nuclear radiation transmission aspects of Gallium (III) trioxide constituting Bi₂O₃-B₂O₃ glasses. *Results Phys* (2021) 30:104899. doi:10.1016/j.rinp.2021.104899
9. Rammah YS, Tekin HO, Sriwunkum C, Olarinoye I, Alalawi A, Al-Buriah MS, et al. Investigations on borate glasses within SBC-Bx system for gamma-ray shielding applications. *Nucl Eng Tech* (2021) 53(1):282–93. doi:10.1016/j.net.2020.06.034

10. Tekin HO, Almisned G, Rammah YS, Ahmed EM, Ali FT, Baykal DS, et al. Transmission factors, mechanical, and gamma ray attenuation properties of barium-phosphate-tungsten glasses: Incorporation impact of WO₃. *Optik* (2022) 267:169643. doi:10.1016/j.ijleo.2022.169643
11. Chandiramouli R, Jeyaprakash BG. Review of CdO thin films. *Solid State Sci* (2003) 16:102–10. doi:10.1016/j.solidstatesciences.2012.10.017
12. Pércio MF, de Campos SD, Schneider R, de Campos EA. Effect of the addition of TiO₂, ZrO₂, V₂O₅ and Nb₂O₅ on the stability parameters of the Li₂O–BaO–SiO₂ glass. *J Non Cryst Sol* (2015) 411:125–31. doi:10.1016/j.jnoncrysol.2014.12.031
13. Gaafar MS, Mahmoud IS. Ultrasonic relaxation of some CdO boro-tellurate glasses. *Can J Phys* (2016) 94(10):1008–16. doi:10.1139/cjp-2016-0363
14. Purohit A, Chander S, Patel SL, Rangra KJ, Dhaka MS. Substrate dependent physical properties of evaporated CdO thin films for optoelectronic applications. *Phys Lett A* (2017) 381(22):1910–4. doi:10.1016/j.physleta.2017.03.049
15. Tekin HO, Kavaz E, Papachristodoulou A, Kamislioglu M, Agar O, Guclu EA, et al. Characterization of SiO₂–PbO–CdO–Ga₂O₃ glasses for comprehensive nuclear shielding performance: Alpha, proton, gamma, neutron radiation. *Ceram Int* (2019) 45(15):19206–22. doi:10.1016/j.ceramint.2019.06.168
16. Kilic G, Ilik E, Issa SAM, Almisned G, Tekin HO. Tailoring critical material properties of some ternary glasses through ZnO/CdO alteration: A focusing study on multiple behavioral changes. *Appl Phys A* (2022) 128:890. doi:10.1007/s00339-022-06040-8
17. Kilic G, Ilik E, Issa SAM, Almisned G, Tekin HO. ZnO/CdO translocation in P₂O₅-TeO₂-ZnO ternary glass systems: A reformative enhancement tool for physical, optical, and heavy-charged particles attenuation properties. *Optik* (2022) 268:169807. doi:10.1016/j.ijleo.2022.169807
18. Kilic G, Kavaz E, Ilik E, Almisned G, Tekin HO. CdO-rich quaternary tellurite glasses for nuclear safety purposes: Synthesis and experimental gamma-ray and neutron radiation assessment of high-density and transparent samples. *Opt Mater* (2022) 129:112512. doi:10.1016/j.optmat.2022.112512
19. Kavaz E, Ilik E, Kilic G, Almisned G, Tekin HO. Synthesis and experimental characterization on fast neutron and gamma-ray attenuation properties of high-dense and transparent Cadmium oxide (CdO) glasses for shielding purposes. *Ceramics Int* (2022) 48(16):23444–51. doi:10.1016/j.ceramint.2022.04.338
20. Biswas R, Sahadath H, Mollah AS, Fazlul Huq M. Calculation of gamma-ray attenuation parameters for locally developed shielding material: Polyboron. *J Radiat Res Appl Sci* (2016) 9(1):26–34. doi:10.1016/j.jrras.2015.08.005
21. Alfuraih AA. Simulation of gamma-ray transmission buildup factors for stratified spherical layers. *Dose Response* (2022) 17(1):155932582110686. doi:10.1177/15593258211070911
22. Hivrekar MM, Sable DB, Solunke MB, Jadhav KM. Different property studies with network improvement of CdO doped alkali borate glass. *J Non Cryst Sol* (2018) 491:14–23. doi:10.1016/j.jnoncrysol.2018.03.051
23. Sindhu S, Sanghi S, Rani S, Agarwal A, Seth VP. Modification of structure and electrical conductivity of cadmium borate glasses in the presence of V₂O₅. *Mater Chem Phys* (2008) 107(2–3):236–43. doi:10.1016/j.matchemphys.2007.07.005
24. Tekin HO. MCNP-X Monte Carlo code application for mass attenuation coefficients of concrete at different energies by modeling 3×3 inch NaI(Tl) detector and comparison with XCOM and Monte Carlo data. *Sci Tech Nucl Installations* (2016) 2016:6547318–7. doi:10.1155/2016/6547318
25. Tekin HO, Almisned G, Issa SAM, Zakaly HMM, Kilic G, Ene A. Calculation of NaI(Tl) detector efficiency using ²²⁶Ra, ²³²Th, and ⁴⁰K radioisotopes: Three-phase Monte Carlo simulation study. *Open Chem* (2022) 20:541–9. doi:10.1515/chem-2022-0169
26. Reda SM, Saleh HM. Calculation of the gamma radiation shielding efficiency of cement-bitumen portable container using MCNPX code. *Prog Nucl Energy* (2021) 142:104012. doi:10.1016/j.pnucene.2021.104012